JCB Article

The J-domain protein Rme-8 interacts with Hsc70 to control clathrin-dependent endocytosis in *Drosophila*

Henry C. Chang, Michael Hull, and Ira Mellman

Department of Cell Biology, Ludwig Institute for Cancer Research, Yale University School of Medicine, New Haven, CT 06520

By screening for mutants exhibiting interactions with a dominant-negative dynamin, we have identified the *Drosophila* homologue of receptor-mediated endocytosis (Rme) 8, a J-domain–containing protein previously shown to be required for endocytosis in *Caenorhabditis elegans*. Analysis of *Drosophila Rme-8* mutants showed that internalization of Bride of sevenless and the uptake of tracers were blocked. In addition, endosomal organization and the distribution of clathrin were greatly disrupted in *Rme-8* cells, suggesting that Rme-8 participates in a clathrin-dependent process. The phenotypes of *Rme-8* mutants bear a strong resemblance to those of *Hsc70-4*, suggesting that these two genes act in a common pathway. Indeed, biochemical and genetic data demonstrated that Rme-8 interacts specifically with Hsc70-4 via its J-domain. Thus, Rme-8 appears to function as an unexpected but critical cochaperone with Hsc70 in endocytosis. Because Hsc70 is known to act in clathrin uncoating along with auxilin, another J-protein, its interaction with Rme-8 indicates that Hsc70 can act with multiple cofactors, possibly explaining its pleiotropic effects on the endocytic pathway.

Introduction

Endocytosis, a process common to all eukaryotic cells, plays a critical role not only in the internalization of extracellular macromolecules, but also in the down-regulation of signaling receptors from the cell surface. One major route of endocytosis is the clathrin-mediated pathway, characterized by the selective internalization of receptors and bound ligands via clathrin-coated vesicles (CCVs; Schmid, 1997; Kirchhausen, 2000). To form CCVs at the plasma membrane, AP-2 adaptors, coat proteins, and clathrin are recruited to coated pits, where the assembly of clathrin into lattice-like structures induces the inward curvature of the membrane. The pits then grow with successive additions of coat proteins, and eventually detach from plasma membrane as CCVs in a dynamin-dependent process. After detachment, the clathrin coats are dissociated from CCVs and are reused for subsequent rounds of endocytosis.

Hsc70, a constitutively expressed member of the Hsp70 chaperone family, has been implicated in many stages of this CCV cycle. In vitro, Hsc70 can promote the release of clathrin triskelions and other coat proteins from CCVs by binding to clathrin and thus disrupting the clathrin cage concomitant with ATP hydrolysis (Schlossman et al., 1984; Chappell et al., 1986; Ungewickell et al., 1995). In addition, Hsc70 can bind to PP2A which, in turn, can modulate the affinity of adaptor complexes for cargo proteins by dephosphorylation (Ghosh and Kornfeld, 2003). Thus, Hsc70 may participate in the release of adaptor proteins, as well as clathrin, from CCVs (Hannan et al., 1998; Ghosh and Kornfeld, 2003). After uncoating, Hsc70 remains associated with clathrin triskelions and may have a role in priming clathrin for future rounds of CCV formation (Schlossman et al., 1984; Jiang et al., 2000). Recent evidence has further suggested that Hsc70, along with its cochaperone auxilin (see next paragraph), binds to dynamin in vitro and may have a role in the early steps of CCV formation (Newmyer et al., 2003).

Despite these advances in understanding the biochemical details of Hsc70 in clathrin-mediated endocytosis, its precise function in vivo remains difficult to demonstrate. That Hsc70 is important in intact cells has been substantiated by experiments perturbing Hsc70 function, either by the expression of dominant-negative mutant alleles (Newmyer and Schmid, 2001) or by selection of Hsc70 mutants in *Drosophila* (Chang et al., 2002). In these examples, inhibition of Hsc70 function under physiological conditions caused defects in clathrin-dependent internalization and in receptor recycling

The online version of this article includes supplemental material.

Address correspondence to Ira Mellman, Dept. of Cell Biology, Ludwig Institute for Cancer Research, Yale University School of Medicine, 333 Cedar Street, PO Box 208002, New Haven, CT 06520-8002. Tel.: (203) 785-4303. Fax: (203) 785-4301. email: ira.mellman@yale.edu

Key words: endocytosis; clathrin; Hsc70; Rme-8; J-domain

Abbreviations used in this paper: Boss, Bride of sevenless; CCV, clathrin-coated vesicle; Clc, clathrin light chain; Hk, Hook; Rme, receptor-mediated endocytosis; *shi*, *shibire*; TR-avidin, Texas red–conjugated avidin.

The Journal of Cell Biology, Volume 164, Number 7, March 29, 2004 1055–1064
http://www.jcb.org/cgi/doi/10.1083/jcb.200311084

The Journal of Cell Biology

(Honing et al., 1994; Morgan et al., 2001; Newmyer and Schmid, 2001; Chang et al., 2002).

Because of the myriad cellular roles of Hsc70, it may be easier to analyze a particular Hsc70 function in vivo by characterizing specific J-domain–containing cochaperones with which it is likely to interact. The J-domain, a conserved motif shared by members of the DnaJ protein family, can bind to Hsp70 family proteins and stimulate their low intrinsic ATPase activity (Ungewickell et al., 1995; Bukau and Horwich, 1998; Kelley, 1999). The relevant cochaperone in the clathrin uncoating reaction is thought to be auxilin, which contains clathrin-binding domains as well as the J-domain (Ungewickell et al., 1995; Umeda et al., 2000). Thus, the proposed mechanism is that auxilin first binds to CCVs, and recruits ATP-bound Hsc70 proteins via its J-domain (Ungewickell et al., 1995; Holstein et al., 1996). The J-domain interaction then stimulates Hsc70 ATPase activity, thereby stabilizing the binding of Hsc70 to clathrin and driving triskelion dissociation (Holstein et al., 1996). Consistent with this, inhibition of auxilin function in vivo causes an accumulation of CCVs, indicative of defects in clathrin uncoating (Gall et al., 2000; Pishvaee et al., 2000; Greener et al., 2001). In addition to auxilin, receptor-mediated endocytosis (Rme) 8, another J-domain–containing protein, was implicated in receptor-mediated internalization and fluid-phase tracer uptake in *Caenorhabditis elegans* (Zhang et al., 2001), suggesting that distinct cochaperones may mediate diverse functions of Hsc70 in endocytosis. However, a link between Rme-8 and Hsc70 has not been established, and the exact role or site of action of Rme-8 remains poorly understood.

To identify new factors regulating endocytosis, we have screened for mutants altering the rough eye phenotype caused by the overexpression of a dominant-negative *shibire* (*shi*), the *Drosophila* homologue of dynamin (van der Bliek and Meyerowitz, 1991; Chang et al., 2002). Mutations in dynamin, a GTPase required for the detachment of CCVs from the plasma membrane, were first isolated as animals exhibiting temperature-sensitive paralysis, caused by a disruption in neurotransmitter recycling (Poodry et al., 1973; Poodry and Edgar, 1979). Although the thermal sensitivity of *shi* has been used to identify other endocytic factors (Narayanan and Ramaswami, 2003), we chose the developing eye for conducting a screen because the rough eye phenotype can detect modifying effects in gradation and is, therefore, more sensitive.

Expression of shi^{K39A}, a GTP hydrolysis–defective dynamin, under the control of eye-specific *GMR* expression cassette has been shown to cause a rough eye phenotype (Chang et al., 2002). Taking advantage of this, we have screened 30,000 progeny and identified several mutations in the *Drosophila* Rme-8 gene. Here, we present evidence suggesting that Rme-8 cooperates with Hsc70-4 and plays a role in regulating clathrin-mediated endocytosis.

Results

E(shi)2-1 is a dominant modifier of a GTP hydrolysis–defective dynamin

Expression of a GTP hydrolysis–defective dynamin, dyn^{K44A}, was shown to block transferrin uptake in HeLa cells (Damke et al., 2001). To test whether this putative dominant-negative dynamin mutant can block endocytosis in *Drosophila* cells, we expressed the fly dynamin homologue *shi* carrying analogous mutation (shi^{K39A}) in eye imaginal discs using the GMR expression cassette (Hay et al., 1994; Chang et al., 2002). The mutant eye discs were then stained with an mAb against Bride of sevenless (Boss; Cagan et al., 1992), and the number of clusters with internalized Boss proteins was counted. Boss encodes the membrane ligand for the Sevenless receptor tyrosine kinase, and is specifically expressed on the apical surface of R8 and internalized into neighboring Sevenless-expressing cells (Cagan et al., 1992). In wild-type discs, 29.6% of the clusters ($n = 1{,}674$) exhibited detectable levels of internalized Boss. In the presence of one copy of $GMR\text{-}shi^{K39A}$, only 18.7% of the clusters ($n = 2{,}000$) contained internalized Boss, and this number was further reduced to 16.7% ($n = 1{,}439$) when two copies of $GMR\text{-}shi^{K39A}$ were expressed. These data suggested that, in fly cells, expression of this GTP hydrolysis–defective dynamin, as in mammalian cells, can dominantly inhibit Rme.

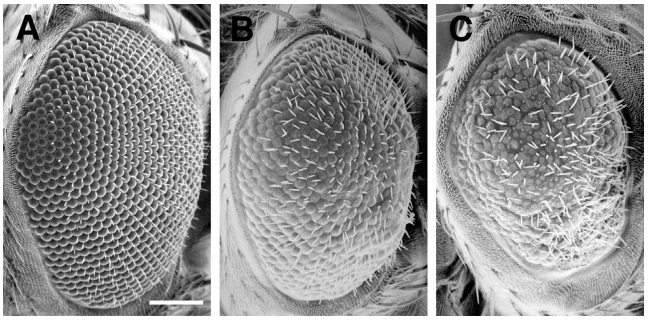

Figure 1. ***E(shi)2-1* enhances the rough eye of a GTP hydrolysis–defective dynamin.** Scanning electron micrographs of the adult eyes of (A) $GMR\text{-}shi^{wt}/+$, (B) $GMR\text{-}shi^{K39A}/+$, and (C) $GMR\text{-}shi^{K39A}/E(shi)2\text{-}1^{A9}$. Anterior is to the right. Bar, 25 μm.

In addition to decreasing the level of Boss internalization, $GMR\text{-}shi^{K39A}$ caused a rough eye phenotype (Fig. 1 B), presumably reflecting an alteration of one or more signaling processes due to the inhibition of endocytosis during eye development (Chang et al., 2002). In contrast, expression of wild-type *shi* using the *GMR* promoter had no effect on eye morphology (Fig. 1 A). As for the Boss internalization defect, the rough eye phenotype became more severe as flies carried more copies of the $GMR\text{-}shi^{K39A}$ transgene (unpublished data). This sensitivity to gene dose suggested that we could use $GMR\text{-}shi^{K39A}$ to identify genes functioning in the dynamin-mediated pathway by isolating second-site mutations that modify (either suppress or enhance) the rough eye phenotype.

Accordingly, we screened ~30,000 x-ray mutagenized progeny for mutants that altered the rough eye phenotype of $GMR\text{-}shi^{K39A}$ (see Materials and methods for details). We isolated 24 enhancers (i.e., those that made the eye phenotype worse) and 1 suppressor (those that made the eye phenotype better), which were assigned into 3 multi-hit and 4 single-hit complementation groups. Here, we describe our characterization of *E(shi)2-1* (17 alleles), which exhibited the strongest enhancer interaction with $GMR\text{-}shi^{K39A}$ among all our mutants (Fig. 1 C).

E(shi)2-1 affects Rme during eye development

The genetic interaction with $GMR\text{-}shi^{K39A}$ suggested that *E(shi)2-1* functions in the endocytic pathway. To test if this

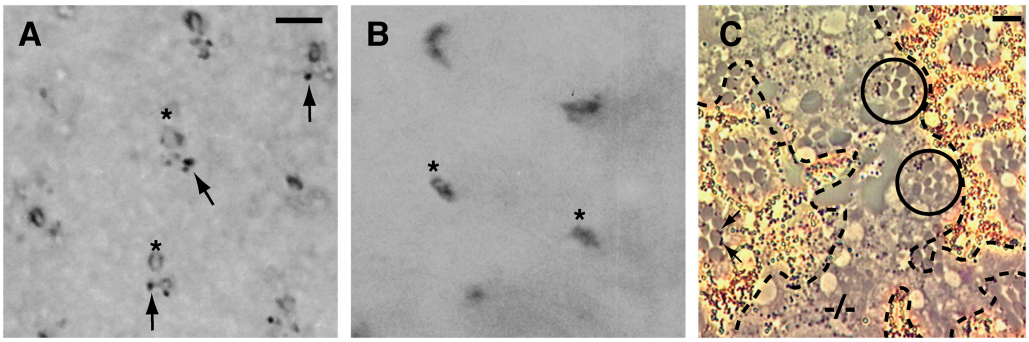

Figure 2. **Receptor-mediated internalization of Boss is defective in *E(shi)2-1* mutant.** Eye discs carrying HRP-Boss dissected from (A) wild-type and (B) *E(shi)2-1*^{A9}/*E(shi)2-1*^{C19} third instar larvae. The Boss proteins on the apical surface of R8 cells are labeled by asterisks, and the Boss internalized by the neighboring cells are indicated by arrows. Note that the accumulations of Boss in neighboring cells are absent in B. (C) A tangential section of an *E(shi)2-1*^{A9} clone in adult retina. Mutant photoreceptor cells are represented by those lacking *white* pigment granules at the base of their rhabdomeres, and delineated by the dash line. *White* pigment granules are the two dark structures (arrows) situated at the bases of rhabdomeres, the light-sensing organelles. Mosaic clusters with a mixture of mutant and wild-type photoreceptors are indicated by circles. In these clusters, the size of rhabdomeres in mutant cells was consistently smaller than those of the wild-type cells. Bars, 5 μm.

was indeed the case, we examined the trafficking of Boss protein in homozygous *E(shi)2-1* mutant tissues during eye development. The localization of Boss proteins can be easily monitored using a functional HRP-Boss chimera in which the cytochemically detectable enzyme HRP was fused to the extracellular domain of Boss (Sunio et al., 1999). In wild-type eye disc (Fig. 2 A), the staining pattern of HRP-Boss fusion was seen as "patches," representing Boss proteins on the apical surface of R8 cells, and "dots," representing those accumulated in structures in Sevenless-expressing cells (Sunio et al., 1999). As shown in Fig. 2 B, the neighboring small dots of HRP-Boss were absent in homozygous *E(shi)2-1* mutant disc, indicating that the receptor-mediated internalization of Boss was inhibited.

In addition to Boss internalization, *E(shi)2-1* was also required for proper ommatidial development. A tangential section of mosaic adult retina showed that mutant clusters often lack complete complement of photoreceptor cells (Fig. 2 C). In mosaic clusters with a normal complement of photoreceptors (Fig. 2 C, circles), the size of rhabdomeres (the light-sensing organelles) in mutant cells was consistently smaller than those of the wild-type cells. Furthermore, the organization of regular ommatidial array in these mutant tissues was disrupted.

E(shi)2-1 inhibits tracer uptake at early steps of the endocytic pathway

To further understand the role of *E(shi)2-1* in the endocytic pathway, we examined the defects in the uptake of an endocytic tracer, Texas red–conjugated avidin (TR-avidin), by homozygous *E(shi)2-1* mutant larval Garland cells. Garland cells are thought to function as nephrocytes and have a rapid rate of fluid-phase endocytosis (Kosaka and Ikeda, 1983). This internalization of TR-avidin by Garland cells appears to be clathrin dependent, as mutations in α-adaptin, a subunit of the AP-2 adaptor complex required for forming CCVs at the plasma membrane (González-Gaitán and Jackle, 1997), inhibit this process (Fig. S3, available at http://www.jcb.org/cgi/content/full/jcb.200311084/DC1). Wild-type and mutant Garland cells were incubated in PBS with TR-avidin for 1 min at 25°C, washed, and then chased for various times (Fig. 3; Videos 1 and 2, available at http://www.jcb.org/cgi/content/full/jcb.200311084/DC1). To identify endocytic compartments, the cells also carried an *Act5C-GAL4/+; UAS-GFP-rab7/+* transgene, which labels late endosomal and lysosomal structures (Entchev et al., 2000). After the 1-min incubation, in wild-type cells most of the TR-avidin was peripherally localized in Rab7-negative structures just beneath the plasma membrane (Fig. 3 A, red). After a chase of 20 min at 25°C, the TR-avidin was transferred to more central regions of the cytoplasm where it was found associated with Rab7-positive structures, suggesting that the tracer had reached late endosomes or lysosomes (Fig. 3 B). In contrast, in *E(shi)2-1/E(shi)2-1* Garland cells, relatively little TR-avidin appeared to be internalized after a 1-min incubation (Fig. 3 D). Moreover, little if any of the tracer was transferred to Rab7-positive structures after a 20-min chase (Fig. 3 E).

To determine whether the small amount of staining seen in *E(shi)2-1/E(shi)2-1* cells represented TR-avidin adsorbed to the plasma membrane or trapped in peripheral intracellular vesicles, the uptake assay was modified so Garland cells without the *GFP-rab7* transgene were incubated in TR-avidin for 1 min at 25°C, chased for 20 min at 25°C, and then incubated with FITC-avidin for 1 min at 4°C. The incubation of second tracer at 4°C allowed us to assess whether TR-avidin had been internalized into compartments inaccessible to outside because further endocytosis would have been inhibited by cold. In wild-type cells (Fig. 3 C), although TR-avidin was seen as vesicular staining near the center, FITC-avidin staining was mostly peripheral near the cell membrane, indicating that TR-avidin has transited to late endocytic compartments after 20 min. In contrast, the staining of TR- and FITC-avidin showed extensive overlap in mutant cells (Fig. 3 F, arrows), indicating that most of the TR-avidin associated with mutant cells was trapped at the plasma membrane or in structures accessible to outside. Although these results could not definitively distinguish whether the tracers were never internalized, or were once internalized but recycled back to the plasma membrane due to a block in transit through endosomal

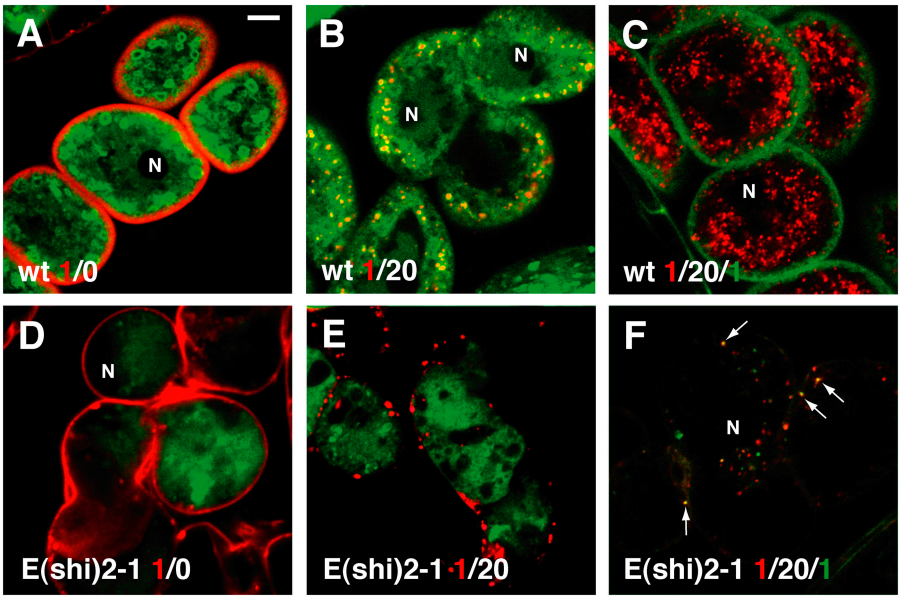

Figure 3. **Tracer uptake is blocked early in the endocytic pathway in *E(shi)2-1* mutant Garland cells.** Uptake of TR-avidin by wild-type (A and B) and *E(shi)2-1*^{A9}/*E(shi)2-1*^{C19} (D and E) Garland cells. Cells were incubated in PBS containing TR-avidin for 1 min and chased for 0 min (A and D) and 20 min (B and E). The cells also expressed a GFP-rab7 fusion to identify late structures in the endocytic pathway. (C and F) Uptake of two waves of tracers by wild-type (C) and *E(shi)2-1*^{A9}/*E(shi)2-1*^{C19} (F) Garland cells. Cells were incubated in PBS containing TR-avidin for 1 min and chased for 20 min at 25°C. Then the cells were chilled on ice, incubated in PBS containing FITC-avidin for 1 min on ice, washed with ice-cold PBS, and fixed. Some overlaps in the staining pattern of the two tracers in F are indicated by arrows. For the sake of consistency, all confocal images of Garland cells shown are those cross sections near the plane of their nuclei (N). Note that these cells are dinucleate. Bar, 5 μm.

compartments, they clearly suggest that *E(shi)2-1* affects endocytosis at some early steps.

Endosomal organization and clathrin distribution are disrupted in *E(shi)2-1* mutant cells

Given that the uptake of the endocytic tracers into Rab7-positive late endosomes was strongly inhibited, we tested whether *E(shi)2-1* exhibited defects in endosomal organization by comparing the staining pattern of Hook (Hk), a cytosolic protein associated with early endosomes (Kramer and Phistry, 1996), and GFP-rab7, in both wild-type and homozygous *E(shi)2-1* mutant tissues. In wild-type Garland cells, Hk was localized to the cell periphery and associated with structures that were distinct from the bulk of the Rab7 staining (Fig. 4 A). In contrast, Hk staining was patchy and greatly reduced in homozygous *E(shi)2-1* Garland cells (Fig. 4 B). In addition, Rab7 appeared more diffuse and centrally located in *E(shi)2-1* Garland cells (Fig. 4 B). Although Rab7-positive structures were still present in *E(shi)2-1* cells, their morphology and density of Rab7 labeling varied considerably.

A defect in Hk localization was also detected in mosaic eye imaginal discs generated by *FLP/FRT* recombination. To identify the z-axis focal plane visualized for each cell cluster, the eye discs were also stained with an anti-Elav antibody, which labels

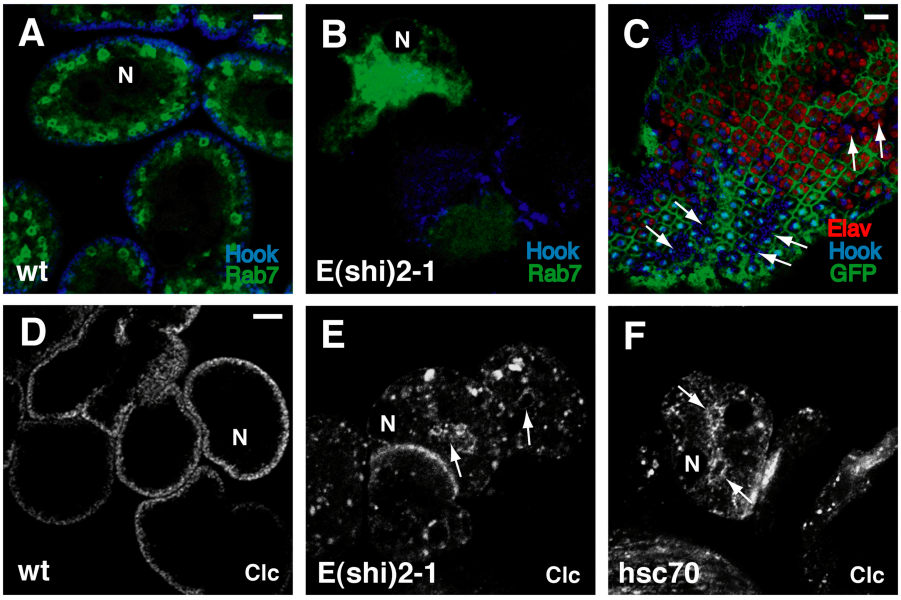

Figure 4. **Clathrin distribution and endosomal organization are disrupted in *E(shi)2-1* mutant Garland cells.** Confocal images of (A) wild-type and (B) *E(shi)2-1*^{A9}/*E(shi)2-1*^{C19} third instar larval Garland cells stained with a rabbit αHk antibody (blue). These cells also carried one copy of the *GFP-rab7* transgene (green). (C) A confocal image of homozygous *E(shi)2-1*^{A9} clones in a mosaic eye disc. The cells were stained with a rabbit αHk antibody (blue) and a rat αElav antibody (red) to label early endocytic structures and nuclei of neuronal cells, respectively. Wild-type cells are indicated by the presence of a membrane-associated GFP expression, whereas mutant cells are indicated by the absence of GFP expression and arrows. Because the disc is slanted, the confocal section of the left side is apical (above the nuclei) and the right side more basal. (D–F) Confocal images of *Clc-GFP* fusion in Garland cells isolated from (D) wild-type, (E) *E(shi)2-1*^{A9}/*E(shi)2-1*^{C19}, and (F) *Hsc70-4*^{R447H}/*Hsc70-4*^{R447H} animals. N, nucleus. Bars: (A, B, and D–F) 5 μm; (C) 15 μm.

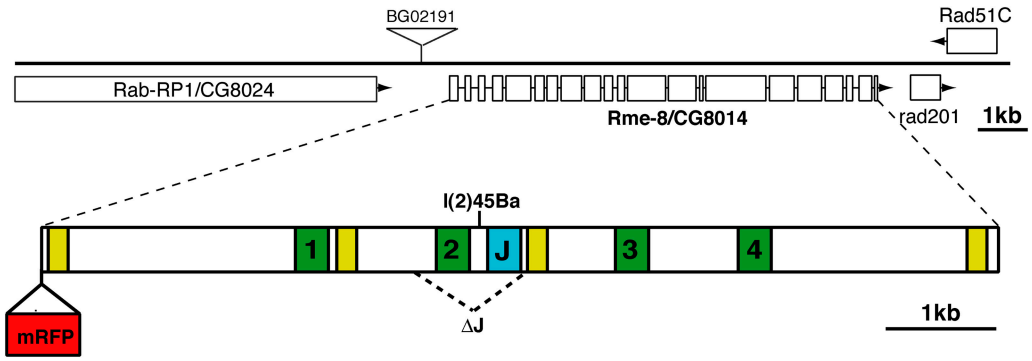

Figure 5. ***E(shi)2-1* encodes *Drosophila* homologue of *Rme-8*.** A schematic representation of the *Drosophila Rme-8/CG8014* locus. The exons of *Rme-8*, flanked by *Rab-RP1* and *rad201* loci, are drawn to scale and shown by white boxes, and the directions of transcription units are indicated by arrows. To test if *E(shi)2-1* corresponds to CG8014, we first generated lethal excision lines from $p\{w^+\}BG02191$ (#12659; Bloomington *Drosophila* stock center), a viable transposon line with a P-element inserted only 92 bp upstream of the CG8014 transcription initiation site. Of the 25 excisions recovered, three were lethal and all failed to complement all alleles of *E(shi)2-1*, suggesting that *E(shi)2-1* is CG8014. This was further confirmed by the sequence analysis of the $E(shi)2\text{-}1^{l(2)45Ba}$ allele, which revealed a premature stop codon before the J-domain in the Rme-8 ORF. Below, a scaled-up diagram of Rme-8 ORF to illustrate the locations of the J-domain (blue box), the four IWN domains (numbered green boxes), and several highly conserved stretches (yellow boxes). To facilitate subsequent analysis of Rme-8 localization, an mRFP (red box) was inserted immediately after the start codon to create a functional mRFP–Rme-8 fusion. To test the importance of its J-domain, a segment, (delineated by the dashed line) including the J- and IWN2 domains, was deleted from Rme-8 to generate mRFP-Rme-$8^{\Delta J}$.

the nuclei of neuronal cells (Robinow and White, 1988). In wild-type cells (indicated by the presence of GFP expression), Hk was concentrated near the apical cortex of photoreceptor cells. In homozygous *E(shi)2-1* mutant cells (indicated by the absence of GFP expression), the staining of Hk proteins appeared more vesicular, less restricted to the apical surface, and could be easily detected at lower focal planes of cells (Fig. 4 C). Together, these data suggested that the organization of endosomal compartments was affected by *E(shi)2-1* mutation.

The genetic interaction with dynamin and the requirement for Boss internalization during eye development suggested that *E(shi)2-1* may play a role in a clathrin-mediated pathway. To determine whether *E(shi)2-1* has an effect on clathrin distribution, we compared the localization of a clathrin light chain-EGFP (Clc-EGFP) in wild-type and mutant Garland cells (Chang et al., 2002). This *Clc-EGFP* was placed under the control of *UAS* regulatory elements, and was expressed in Garland cells using the *Act5C-GAL4* driver line. In wild-type cells, Clc-EGFP was seen as punctate staining around the cell periphery, presumably representing vesicular clathrin-coated structures (Fig. 4 D). However, in homozygous *E(shi)2-1* cells, the Clc-EGFP staining was weaker and more diffuse, although clustering near the limiting membrane of some large internal structures was occasionally observed (Fig. 4 E, arrows). This abnormal distribution of Clc-EGFP in mutant Garland cells suggested that clathrin function may be compromised by *E(shi)2-1*. Interestingly, the phenotype of clathrin mislocalization, as well as those defects in endosomal organization, were remarkably similar to those seen in cells deficient in *Hsc70-4*, the *Drosophila* homologue of clathrin uncoating ATPase (Fig. 4 F; Chang et al., 2002), raising the possibility that *E(shi)2-1* and *Hsc70-4* function in a common pathway.

E(shi)2-1 encodes fly homologue of *Rme-8* gene

To identify the gene responsible for *E(shi)2-1*, the enhancement of the $GMR\text{-}shi^{K39A}$ rough eye was first mapped to 2-61 ($n = 62$) by meiotic recombination. The lethality associated with *E(shi)2-1* was included in the deletion *Df(2R)G63-73* (45A13-B1;45D5-8) but excluded from *Df(2R)w73-3* (45B5-7;45D5-8), placing the gene in the cytological interval of 45A13-B1 to B5-7. The position of gene was further narrowed down to a region between two P-element lines, *l(2)k04512* and *l(2)k06021* (Spradling et al., 1995, 1999), using P-element–mediated male recombination (Chen et al., 1998).

Although there are ~13 transcriptional units between *l(2)k04512* and *l(2)k06021*, we decided to focus on large transcripts first because 17 alleles of *E(shi)2-1* were isolated from a relatively small screen, suggesting that the *E(shi)2-1* coding region is large. Indeed, sequencing analysis of $E(shi)2\text{-}1^{l(2)45Ba}$ revealed that *CG8014* (Berkeley *Drosophila* Genome Project; Rubin et al., 2000), the largest transcript in the region (ORF = 7,162 bp), contained a nonsense mutation at tryptophan[1287] (Fig. 5). Consistent with this interpretation, ubiquitous expression of *CG8014* under the *Act5C-GAL4* driver could revert the enhancement of the $GMR\text{-}shi^{K39A}$ rough eye phenotype by *E(shi)2-1* alleles, and could rescue the recessive lethality associated with *E(shi)2-1* (unpublished data). Together, these observations indicate that *CG8014* is the gene for *E(shi)2-1*. Expression profile analysis from the Berkeley *Drosophila* Genome Project indicated that *CG8014* transcripts were detected ubiquitously throughout all stages of embryonic development, but enriched in Malpighian tubule and Garland cells (Tomancak et al., 2002).

CG8014 encodes a protein of 2,387 amino acids, most homologous to *Rme-8*, a gene previously identified in *C. elegans* for defects in Rme (Zhang et al., 2001). Putative homologues were also found in *Arabidopsis* (GenBank/EMBL/DDBJ accession no. NP_180257), rice (AAP55138), rat (XP_236584), and human (BK001645), suggesting that the function of Rme-8 is conserved (Zhang et al., 2001). Although no obvious motif except an internal J-domain was

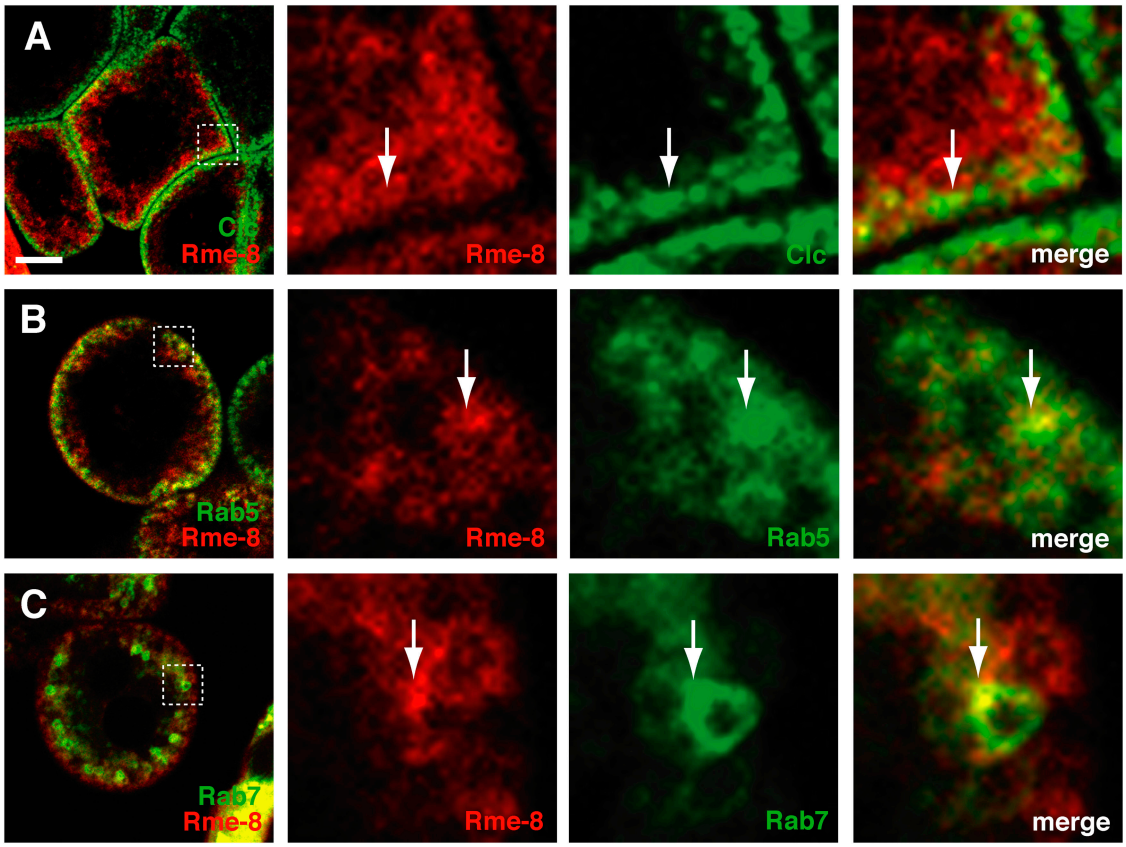

Figure 6. **Rme-8 proteins are associated with multiple endosomal structures.** Confocal micrographs of Garland cells expressing mRFP-tagged Rme-8 (red) and various subcellular protein markers (green). The genotypes of these cells are (A) *Act5C-GAL4/UAS-mRFP-Rme-8^{FL}*;UAS-Clc-EGFP-C1/+, (B) *Act5C-GAL4/UAS-mRFP-Rme-8^{FL};UAS-GFP-Rab5*/+, and (C) *Act5C-GAL4/UAS-mRFP-Rme-8^{FL};UAS-GFP-Rab7*/+. The boxed regions are shown in high magnification. The regions where Rme-8 shows spatial overlaps with various markers are indicated by arrows. Bar, 5 μm.

detected in Rme-8 protein sequence, comparison of Rme-8 sequences from divergent species revealed four previously defined IWN domains (Zhang et al., 2001) and several conserved regions (Fig. 5). The functions of these domains are not known; however, the high degree of conservation does suggest that they are critical for Rme-8.

Rme-8 proteins are associated with multiple endocytic structures

Although the *C. elegans* Rme-8 proteins appeared to be associated with some multivesicular compartments, the identities of these structures were not established (Zhang et al., 2001). To determine the subcellular localization of Rme-8 proteins, we constructed *UAS-mRFP-Rme-8^{FL}*, where a full-length *Rme-8* genomic/cDNA fusion is tagged at the NH_2 terminus with a monomeric RFP (Campbell et al., 2002; Fig. 5). Ubiquitous expression of this construct could counter the enhancement of the *GMR-shi^{K39A}* rough eye phenotype by loss-of-function *Rme-8* mutations (unpublished data), indicating that this *mRFP-Rme-8^{FL}* was functional.

To help in identifying subcellular structures, *Act5C-GAL4/+;UAS-mRFP-Rme-8^{FL}/+* Garland cells also carried one copy of *UAS-Clc-GFP*, *UAS-GFP-rab5*, or *UAS-GFP-rab7* transgene (Entchev et al., 2000; Chang et al., 2002; Wucherpfennig et al., 2003). Clc, Rab5, and Rab7 are markers for clathrin-positive organelles, early endosomes, and late endosomes, respectively. Although most of the Rme-8 appeared to be cytosolic, accumulating beneath the plasma membrane, there were some spatial overlaps with clathrin-, Rab7-, and Rab5-positive structures (Fig. 6). Rme-8 also exhibited some spatial overlaps with Hrs, a protein required for endosomal invagination (Lloyd et al., 2002; Fig. S1, available at http://www.jcb.org/cgi/content/full/jcb.200311084/DC1). These data suggested that Rme-8 proteins were associated with multiple endocytic compartments.

Rme-8 exhibits genetic interaction with Hsc70

Although the presence of a J-domain suggests that Rme-8 might act as an accessory factor for Hsc70, this possibility has not been addressed experimentally. To determine if the two proteins interact functionally in vivo, an ATP hydrolysis–defective Hsc70-4 (Hsc70-4^{K71S}) was expressed in the eye discs using the *GMR-GAL4* driver (Elefant and Palter, 1999). Expression of a mammalian Hsc70 carrying the analogous mutation in HeLa cells was shown to inhibit transferrin internalization and recycling, suggesting the mutant can interfere with the functions of endogenous wild-type Hsc70 (Newmyer and Schmid, 2001). Similarly, expression of Hsc70-4^{K71S} during eye development caused a disruption of the regular arrays of ommatidia and a

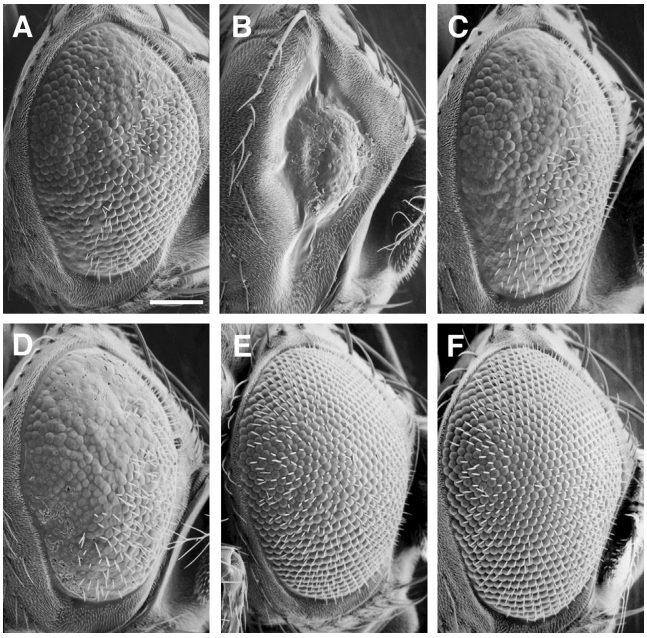

Figure 7. **Rme-8 exhibits specific genetic interactions with Hsc70-4.** Scanning electron micrographs of the adult eyes of (A) *+/+;GMR-GAL4/UAS-Hsc70-4^{K71S}*, (B) *UAS-Rme-8^{FL}/+;GMR-GAL4/UAS-Hsc70-4^{K71S}*, (C) *UAS-Rme-8$^{\Delta J}$/+;GMR-GAL4/UAS-Hsc70-4^{K71S}*, (D) *UAS-Aux/+;GMR-GAL4/UAS-Hsc70-4^{K71S}*, (E) *+/+;GMR-GAL4/UAS-Hsc70-3^{K97S}*, and (F) *UAS-Rme-8^{FL}/+;GMR-GAL4/UAS-Hsc70-3^{K97S}*. Anterior is to the right. Bar, 25 μm.

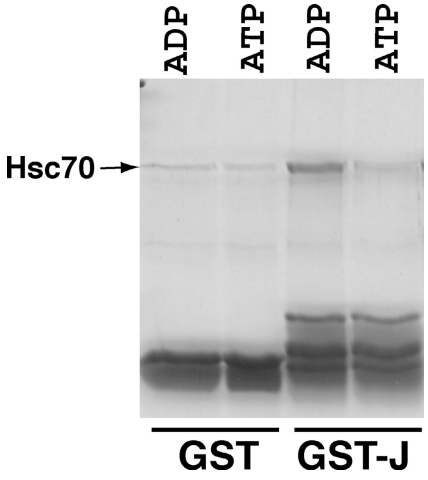

Figure 8. **The J-domain of Rme-8 can bind to Hsc70 in the presence of ADP in vitro.** Bovine Hsc70 proteins were incubated with GST-J^{Rme-8} (GST-J) and GST for 15 min at 37°C under the indicated nucleotide conditions. Bound Hsc70 (arrow) was then analyzed with SDS-PAGE.

roughening of the eye (Fig. 7 A). Coexpression of mRFP-Rme-8^{FL} using the *GMR-GAL4* driver caused further ommatidial disorganization and a decrease in eye size (Fig. 7 B), indicating that the rough eye phenotype of *Hsc70-4^{K71S}* was enhanced by *Rme-8* expression. Because overexpression of this functional *mRFP-Rme-8^{FL}* alone has no obvious phenotype, this enhancement of *Hsc70-4^{K71S}* suggests that *Rme-8* genetically interacts with *Hsc70-4*. Moreover, the directionality of this interaction suggests that *Rme-8* acts antagonistically with *Hsc70*.

To confirm that this genetic interaction is mediated by the J-domain, Rme-8 with its internal J-domain deleted (mRFP-Rme-8$^{\Delta J}$; Fig. 5) was coexpressed with Hsc70-4^{K71S} using a *GMR-GAL4* driver (Fig. S2, available at http://www.jcb.org/cgi/content/full/jcb.200311084/DC1). In contrast to full-length Rme-8, expression of Rme-8$^{\Delta J}$ had little effect on the *Hsc70-4^{K71S}* phenotype (Fig. 7 C), suggesting that the enhancement by full-length *Rme-8* requires its J-domain.

To demonstrate the specificity of this *Rme-8–Hsc70* interaction, we also coexpressed a full-length auxilin with Hsc70-4^{K71S} during eye development. Surprisingly, although the J-domain–containing auxilin has been shown to cooperate in Hsc70-mediated uncoating of CCVs in vitro, its expression has little or no effect on the rough eye phenotype of Hsc70-4^{K71S} (Fig. 7 D). This contrast in *Hsc70* interaction between *auxilin* and *Rme-8* suggests that they are functionally distinct. Conversely, an ATP hydrolysis–defective Hsc70-3 (Hsc70-3^{K97S}) was expressed in the eye discs using the *GMR-GAL4* driver to test whether the enhancement by *Rme-8* was specific to *Hsc70-4*. Hsc70-3 is the *Drosophila* homologue of BiP, an ER-associated Hsc70 required for translocation of newly synthesized membrane proteins (Elefant and Palter, 1999). Expression of this dominant-negative Hsc70-3^{K97S} during eye development caused a slight deformation and roughening of the eye (Fig. 7 E). Coexpression of a full-length Rme-8 using the *GMR-GAL4* driver exhibited little or no effect on the *Hsc70-3^{K97S}* phenotype (Fig. 7 F), suggesting that Rme-8 cooperates with Hsc70-4, but not other Hsc70 family proteins.

The J-domain of Rme-8 binds to Hsc70 in the presence of ADP in vitro

To determine whether the J-domain of Rme-8 can bind to Hsc70 directly, a peptide (aa 1301–1368) containing the J-domain of the *Drosophila Rme-8* was fused to GST, and the resulting fusion, GST-J^{Rme-8}, was subjected to a pull-down assay with bovine Hsc70. It is generally thought that J-domains recruit ATP-bound Hsc70 (Kelley, 1999), thus the pull-down was performed in either the presence of ATP or ADP to see if the binding was nucleotide dependent. Surprisingly, although GST-J^{Rme-8} exhibited the same level of binding as GST alone in the presence of ATP, GST-J^{Rme-8} showed an elevated level of binding to bovine Hsc70 in the presence of ADP (Fig. 8). Thus, unlike the J-domain from auxilin, the J-domain of Rme-8 appears to interact with ADP-bound Hsc70. These data, along with the enhancement by *Rme-8* overexpression of the mutant rough eye phenotype due to dominant-negative *Hsc70*, suggest that the interaction of Rme-8 with Hsc70 may be different from that of other J-domain–containing proteins.

Discussion

We have isolated mutations in the *Drosophila Rme-8* gene from a screen for mutants exhibiting interactions with a GTP hydrolysis–defective dynamin. Consistent with this genetic interaction, phenotypic analysis suggests that Rme-8 is required for the internalization of membrane ligands and endocytic tracers. Our data, along with the previous analysis of

C. elegans Rme-8 (Zhang et al., 2001) and the high degree of sequence conservation among Rme-8 homologues from divergent species, strongly support the notion that Rme-8 is an evolutionarily conserved factor in endocytosis.

In *C. elegans* coelomocytes, Rme-8 proteins appeared to be associated with the membrane of some large multivesicular endosomal structures, although the identity of these structures was unclear (Zhang et al., 2001). In *Drosophila* Garland cells, the functional mRFP-tagged Rme-8 proteins appeared to be associated with multiple endocytic organelles including clathrin-, Rab5-, and Rab7-positive structures. This, along with the abnormal Clc, Hk, and Rab7 staining exhibited by *Rme-8* mutants, might suggest that Rme-8 has a role in organizing and/or maintaining endosomal compartments. Disrupting the integrity of these endosomal compartments by *Rme-8* mutations may cause a depletion of the cytosolic clathrin pool, which leads to the apparent block in the uptake of endocytic tracers. Alternatively, Rme-8 may have a more direct role at some early steps of endocytosis. The strong inhibition of tracer uptake and the genetic interaction with dynamin exhibited by *Rme-8* mutants are certainly consistent with this possibility. Still, the understanding of the mechanisms of Rme-8 function would require the identification and characterization of its binding partners.

In any case, it seems clear that Rme-8 acts as an unexpected cofactor specific for Hsc70-4 in clathrin-mediated endocytosis. First, the mutant phenotypes of *Rme-8*, such as defects in Boss internalization, uptake of endocytic tracers, endosomal organization, and clathrin distribution, are remarkably similar to those of *Hsc70-4* (Chang et al., 2002). Actually, the phenotypic resemblance appears to extend beyond defects in endocytosis as homozygous *Rme-8* animals, like *Hsc70-4* mutants, are developmentally delayed and often contain melanotic masses (unpublished data). However, the most compelling evidence is that *Rme-8* exhibited a J-domain–dependent genetic interaction with *Hsc70-4*, but not with other members of Hsc70 family proteins. The in vitro pull-down assay further showed that the J-domain of Rme-8 could bind to Hsc70, suggesting that the Hsc70–Rme-8 interaction is likely to be direct. These data, along with the vast similarities in phenotypes exhibited by *Rme-8* and *Hsc70-4* mutants, strongly argue that the internal J-domain is critical for Rme-8 to regulate Hsc70 function.

The observation that overexpression of a functional Rme-8 has an inhibitory effect on a dominant-negative Hsc70 suggests that Rme-8 acts antagonistically to Hsc70 during endocytosis. This, along with the binding of the Rme-8 J-domain to ADP-bound Hsc70, suggests that Rme-8 may act as an inhibitor of the Hsc70 ATPase cycle. One proposed mechanism for this dominant-negative behavior of $Hsc70^{K71S}$ is that the mutant protein fails to release substrates upon ATP binding (Elefant and Palter, 1999). Thus, the *GMR-Hsc70*^{K71S} rough eye phenotype could be caused by the sequestration of limited substrates or effectors. Although the J-domain of Rme-8 does not appear to bind to ATP-bound Hsc70, it is conceivable that overexpression of full-length Rme-8 may interact with the endogenous wild-type ADP-bound Hsc70 and cause a further sequestration of relevant substrates, thereby enhancing the *Hsc70*^{K71S} eye phenotype.

In any event, although Rme-8 interacts with Hsc70 to regulate clathrin-dependent endocytosis, several evidences suggest that Rme-8 is not itself involved in clathrin uncoating. First, the strong endocytic phenotypes of *Hsc70*^{R447H}, a point mutation with a moderate reduction in uncoating activity, were recapitulated by *Rme-8* mutations, suggesting *Rme-8* mutations affected some Hsc70-dependent processes distinct from uncoating. Consistent with this, inspection of the Rme-8 sequence does not reveal any clathrin-binding sites (Morgan et al., 2000). Furthermore, overexpression of auxilin and Rme-8 exhibit different genetic interactions with Hsc70. Together, these data suggest that Rme-8 most likely participates in some novel processes in Hsc70-mediated endocytosis. Thus, by establishing a link between Rme-8 and Hsc70, our data strongly suggest that the function of Hsc70 in endocytosis in vivo is more complex and probably not limited to clathrin uncoating. Although a more extensive role for Hsc70 has been implied by the observation that a decrease in Hsc70 function caused multiple defects in the endocytic pathway, such as the recycling of transferrin (Newmyer and Schmid, 2001; Chang et al., 2002), it has remained unclear whether the associated defects reflected distinct functions of Hsc70 as opposed to indirect consequences of a block in clathrin uncoating. Our identification of a second J-domain cochaperone that is critical for endocytosis is certainly consistent with the pleiotropic effects of Hsc70 on the endocytic pathway. Conceivably, the interaction of the clathrin-binding protein auxilin with Hsc70 is selectively important for coated vesicle uncoating, and the Rme-8–dependent function of Hsc70 might control a downstream step. In either event, the identification of Rme-8 as a second cofactor for Hsc70 in endocytosis should provide a framework for further understanding the diverse functions of Hsc70 in this process.

Materials and methods

Fly genetics

All fly crosses were performed at 25°C in standard laboratory conditions. For the *GMR-shi*^{K39A} modifier screen, *w; iso 2; 3* males were mutagenized with 4,000 rad of x-ray irradiation, and were mass mated with *w/w; TM3, Sb, P{w*$^{+}$*, GMR-shi*^{K39A}*}-3/e, ftz. ry* virgins. Progeny exhibiting altered *GMR-shi*^{K39A} eye phenotype were individually backcrossed to *w/w; TM3, Sb, P{w*$^{+}$*, GMR-shi*^{K39A}*}-3/e, ftz. ry* flies to ensure the phenotype bred true. Based on the segregation of *GMR-shi*^{K39A} modifying phenotype, the putative mutants were then maintained over appropriate balancers, and were grouped by complementation tests.

All of our Rme-8 alleles appear to be recessive embryonic lethal. However, mutant animals trans-heterozygous for certain allelic combinations, such as *Rme-8*^{A9}*/Rme-8*^{C19}, do reach larval stages as rare escapers, allowing isolation of mutant eye discs and larval Garland cells for the *HRP-Boss* and tracer uptake analysis.

For the tangential section of adult retina, mitotic mutant clones were generated by heat-shocking progeny from crosses between *w; FRT*^{neo}42D, *Rme-8*^{A9} males and *hs-FLP1; FRT*^{neo}42D, P{w^{+}}*47A* females (Xu and Rubin, 1993). Mitotic clones in larval eye discs were generated using *ey-FLP; FRT42D*^{neo}*, GMR-myrGFP-2R* (Chang et al., 2002).

To facilitate exogenous protein expression in larval Garland cells, UAS-derived transgenes (*UAS-mRFP-Rme-8*, *UAS-GFP-rab5*, *UAS-GFP-rab7*, and *UAS-GFP-Clc*) were driven with *Act5C-GAL4* (#4414; Bloomington *Drosophila* stock center). For the *Rme-8–Hsc70* interaction tests, *UAS-Hsc70-4*^{K71S} and *UAS-Hsc70-3*^{K97S} (Elefant and Palter, 1999) were expressed during eye development by *GMR-GAL4*. *UAS-GFP-rab5* and *UAS-GFP-rab7* flies were obtained from M.A. González-Gaitán (Max Planck Institute of Molecular Cell Biology and Genetics, Dresden, Germany). *UAS-Hsc70-4*^{K71S}, *UAS-Hsc70-3*^{K97S}, and *GMR-GAL4* were obtained from the Bloomington *Drosophila* stock center.

Genetic mapping of Rme-8

To clone *E(shi)2-1*, the mutation was first placed in the cytological interval of 45B1 to B7 between two P-element lines, *l(2)k04512* (#10544; Bloomington *Drosophila* stock center) and *l(2)k06021* (Bloomington *Drosophila* stock center; see text for details). This region has been subjected to an extensive F_2 genetic analysis (Dockendorff et al., 2000), and complementation tests showed that *E(shi)2-1* is allelic with *l(2)45Ba*. Consistent with this, *l(2)45Ba* also exhibited a strong interaction with *GMR-shi*^{K39A}.

Of all the transcription units in the region between *l(2)k04512* and *l(2)k06021*, *CG8014* is the largest one. To test if *E(shi)2-1* corresponds to *CG8014*, we first generated lethal excision lines from *p{w*$^{+}$*}BG02191* (#12659; Bloomington *Drosophila* stock center), a viable transposon line with a P-element inserted only 92 bp upstream of *CG8014* transcription initiation site. Of the 25 excisions recovered, three were lethal, suggesting that the *CG8014* locus might have been disrupted. All three lethal excision lines exhibited strong interaction with *GMR-shi*^{K39A} and failed to complement all alleles of *E(shi)2-1*, suggesting that *E(shi)2-1* is *CG8014*. To confirm this was indeed the case, exons of *CG8014* locus were amplified by PCR from the genomic DNA of *E(shi)2-1*$^{l(2)45Ba}$*/+* heterozygous animals, and were subjected to sequence analysis.

Histology and immunohistochemistry

For the visualization of HRP-Boss, eye discs dissected from third instar larvae were stained in PBS containing 0.5 mg/ml DAB and 0.003% H_2O_2 for 30 min at RT (Sunio et al., 1999). The discs were then washed twice with PBS and fixed in 2% glutaraldehyde/PBS for 40 min at 4°C. After two washes with PBS, the discs were mounted in 80% glycerol/PBS.

For the endocytic tracer uptake assay, dissected Garland cells were incubated in PBS containing 0.2 mg/ml TR-avidin (A-821; Molecular Probes, Inc.) for 1 min at 25°C. The cells were then washed with PBS, chased, and fixed with 4% PFA/PBS for 20 min at 4°C.

For the double-endocytic tracer uptake assay, dissected Garland cells were incubated in PBS containing 0.2 mg/ml TR-avidin for 1 min at 25°C. Then, the cells were washed with PBS, chased for 20 min, and chilled on ice. Finally, they were incubated in PBS containing 0.2 mg/ml FITC-conjugated avidin (A-820; Molecular Probes, Inc.) for 1 min at 4°C, washed with ice-cold PBS, and fixed with 4% PFA/PBS for 20 min at 4°C.

Immunostaining of eye discs and Garland cells was performed according to Wolff (2000). Rabbit polyclonal anti-Hk antibody (a gift from H. Kramer, University of Texas Southwestern, Dallas, TX) was used at 1:500 dilution (Kramer and Phistry, 1996), and rat anti-Elav antibody (Developmental Studies Hybridoma Bank, Iowa City, IA) was used at 1:100 dilution. All confocal microscopy was performed using a microscope (Axiovert S100-TV; Carl Zeiss MicroImaging, Inc.) with a confocal system (MRC 1024; Bio-Rad Laboratories).

Scanning EM

Scanning EM was performed as described previously (Wolff, 2000). In brief, the eyes were fixed and dehydrated through a graded ethanol series (25, 50, 75, and 2× 100%). The samples were then incubated in hexamethyldisilazane (Sigma-Aldrich), dried under vacuum overnight, mounted on stubs, and imaged with a scanning electron microscope (model SS40; International Scientific Instruments).

Molecular biology

Because of its relatively large size, no complete *Drosophila Rme-8* cDNA was available from the Berkeley *Drosophila* Genome Project EST collection, as LD15941, the longest EST clone of *Rme-8*, covered only the COOH-terminal 3.2 kb. To construct a full-length Rme-8 transcription unit, three fragments corresponding to the NH_2-terminal, central, and COOH-terminal regions of *Rme-8* were individually amplified by PCR and sequentially subcloned into pBlueScript® SK (pBSSK; Strategene). First, an mRFP ORF without the stop codon was PCR amplified from pRSETB-mRFP1 (Campbell et al., 2002) using 5′-GCGAATTCATGGCCTCCTCCGAGGACGTC-3′ and 5′-GCATCGATGGCGCCGGTGGAGTGGCGGC-3′, and subcloned as an EcoRI–ClaI fragment into pHFK to make pHFK-mRFP-RC. The NH_2-terminal portion of Rme-8 was generated by PCR from genomic DNA using 5′-GCCATCGATCTGCCGCCTAAGGAAAACG-3′ and 5′-GCACTCTAGAATGGTTACATTACCAC-3′, and subcloned in frame as a 2.6-kb ClaI–XbaI fragment into pHFK-mRFP-RC. This mRFP-Rme-8 NH_2 terminus fusion was then excised as a NotI–XbaI fragment and subcloned into pBSSK to make pBSSK-mRFP-Rme-8^{1st}. Next, the central portion of Rme-8 was amplified from genomic DNA using 5′-GACAACCCATGTGGTAATGTAAC-3′ and 5′-GATGCCGTTCGCTGCTGCTCGAGG-3′, and subcloned into pBSSK-mRFP-Rme-8^{1st} as an XbaI–XhoI fragment to make pBSSK-mRFP-Rme-8$^{1st+2nd}$. Finally, the COOH-terminal portion of Rme-8 was amplified from LD15941 using 5′-CGCGCTCAGCTTAAGGATTTC-3′ and 5′-GCGCTCGAGCGGCCGCTACGCTTTGCGCAGGACCCGC-3′ to engineer a NotI site after the stop codon, but before the XhoI site. The resulting 1.9-kb PCR products were subcloned as an XhoI fragment into pBSSK-mRFP-Rme-8$^{1st+2nd}$ to complete the construction (pBSSK-mRFP-Rme-8^{FL}). The entire transcription unit was then verified by direct sequencing, and subcloned as a NotI fragment into pUAST expression vector (Brand and Perrimon, 1993). To make the J-domain deletion derivative, a BspEI fragment (corresponding to aa 1114–1385) was excised from the central XbaI–XhoI fragment before being subcloned into pBSSK-mRFP-Rme-8^{1st}.

To construct pGMR-auxilin, a DNA fragment containing the entire auxilin (CG1107) ORF was excised from GH26573 (Research Genetics) as an EcoRI–XhoI fragment with the XhoI end blunted, and subcloned into the EcoRI–HpaI sites of pGMR (Hay et al., 1994). Transgenic flies carrying these constructs were generated by P-element–mediated transformation as described previously (Rubin and Spradling, 1982).

To construct GST-J^{Rme-8}, a DNA fragment containing the J-domain was generated by PCR using primers 5′-GAATTCGCTTACCAGGACCTAGGG-3′ and 5′-CTCGAGGGGATCTGGCCCACCCGAGCTCC-3′. The resulting product was subcloned as an EcoRI–XhoI fragment into pGEX-6P.

Rme-8 J-domain pull-downs

In a total volume of 20 μl, 4 μM GST-J^{aux} was incubated for 15 min at 25°C with 4 μM Hsc70 protein and 2 mM nucleotide in uncoating buffer containing 0.1% ovalbumin and 125 mM KCl. The binding reaction was transferred to 4°C and incubated with 20 μl GSH-Sepharose (50% slurry) with shaking for 30 min. The beads were collected by centrifugation at 16,000 *g* and washed twice with ice-cold buffer containing the appropriate nucleotide (0.1 mM). The bound material was then analyzed by SDS-PAGE.

Online supplemental material

Fig. S1 showed the spatial overlaps between the localization of Rme-8 and Hrs (Lloyd et al., 2002) proteins in larval Garland cells. Fig. S2 showed the in vivo expressions of various mRFP-tagged Rme-8 constructs in larval eye imaginal discs. Fig. S3 showed the uptake of TR-avidin (A-821; Molecular Probes, Inc.) by α-adaptin mutant Garland cells (González-Gaitán and Jackle, 1997). Videos 1 and 2 showed the uptake of TR-avidin by wild-type and Rme-8 mutant Garland cells, respectively, using time-lapse confocal microscopy. Live Garland cells carrying GFP-rab7 transgenes were dissected and mounted in PBS containing 0.2 mg/ml TR-avidin. Confocal images of these cells were captured at a 10-s interval for 10 min, and were then processed by GraphicConverter software (4 frames/s; Lemke Software). Online supplemental material available at http://www.jcb.org/cgi/content/full/jcb.200311084/DC1.

We would like to thank Marcos A. González-Gaitán for providing fly strains, Sherri Newmyer (University of California, San Francisco, San Francisco, CA) for providing bovine Hsc70 proteins, and Helmut Kramer for providing anti-Hk antibody. We also thank members of the Mellman/Warren laboratory for their interest and advice.

This work was supported by National Institutes of Health grant GM29765 and by the Ludwig Institute for Cancer Research. H. Chang was a fellow of the Damon Runyon-Walter Winchell Cancer Research Foundation.

Submitted: 17 November 2003
Accepted: 17 February 2004

References

Brand, A.H., and N. Perrimon. 1993. Targeted gene expression as a means of altering cell fates and generating dominant phenotypes. *Development.* 118:401–415.

Bukau, B., and A.L. Horwich. 1998. The Hsp70 and Hsp60 chaperone machines. *Cell.* 92:351–366.

Cagan, R.L., H. Kramer, A.C. Hart, and S.L. Zipursky. 1992. The bride of sevenless and sevenless interaction: internalization of a transmembrane ligand. *Cell.* 69:393–399.

Campbell, R.E., O. Tour, A.E. Palmer, P.A. Steinbach, G.S. Baird, D.A. Zacharias, and R.Y. Tsien. 2002. A monomeric red fluorescent protein. *Proc. Natl. Acad. Sci. USA.* 99:7877–7882.

Chang, H.C., S.L. Newmyer, M.J. Hull, M. Ebersold, S.L. Schmid, and I. Mellman. 2002. Hsc70 is required for endocytosis and clathrin function in *Drosophila*. *J. Cell Biol.* 159:477–487.

Chappell, T.G., W.J. Welch, D.M. Schlossman, K.B. Palter, M.J. Schlesinger, and J.E. Rothman. 1986. Uncoating ATPase is a member of the 70 kilodalton

family of stress proteins. *Cell.* 45:3–13.

Chen, B., T. Chu, E. Harms, J.P. Gergen, and S. Strickland. 1998. Mapping of *Drosophila* mutations using site-specific male recombination. *Genetics.* 149: 157–163.

Damke, H., D.D. Binns, H. Ueda, S.L. Schmid, and T. Baba. 2001. Dynamin GTPase domain mutants block endocytic vesicle formation at morphologically distinct stages. *Mol. Biol. Cell.* 12:2578–2589.

Dockendorff, T.C., S.E. Robertson, D.L. Faulkner, and T.A. Jongens. 2000. Genetic characterization of the 44D-45B region of the *Drosophila melanogaster* genome based on an F2 lethal screen. *Mol. Gen. Genet.* 263:137–143.

Elefant, F., and K.B. Palter. 1999. Tissue-specific expression of dominant negative mutant *Drosophila* HSC70 causes developmental defects and lethality. *Mol. Biol. Cell.* 10:2101–2117.

Entchev, E.V., A. Schwabedissen, and M. González-Gaitán. 2000. Gradient formation of the TGF-β homolog Dpp. *Cell.* 103:981–991.

Gall, W.E., M.A. Higginbotham, C. Chen, M.F. Ingram, D.M. Cyr, and T.R. Graham. 2000. The auxilin-like phosphoprotein Swa2p is required for clathrin function in yeast. *Curr. Biol.* 10:1349–1358.

Ghosh, P., and S. Kornfeld. 2003. AP-1 binding to sorting signals and release from clathrin-coated vesicles is regulated by phosphorylation. *J. Cell Biol.* 160: 699–708.

González-Gaitán, M., and H. Jackle. 1997. Role of *Drosophila* α-adaptin in presynaptic vesicle recycling. *Cell.* 88:767–776.

Greener, T., B. Grant, Y. Zhang, X. Wu, L.E. Greene, D. Hirsh, and E. Eisenberg. 2001. *Caenorhabditis elegans* auxilin: a J-domain protein essential for clathrin-mediated endocytosis in vivo. *Nat. Cell Biol.* 3:215–219.

Hannan, L.A., S.L. Newmyer, and S.L. Schmid. 1998. ATP- and cytosol-dependent release of adaptor proteins from clathrin-coated vesicles: A dual role for Hsc70. *Mol. Biol. Cell.* 9:2217–2229.

Hay, B.A., T. Wolff, and G.M. Rubin. 1994. Expression of baculovirus P35 prevents cell death in *Drosophila*. *Development.* 120:2121–2129.

Holstein, S.E., H. Ungewickell, and E. Ungewickell. 1996. Mechanism of clathrin basket dissociation: separate functions of protein domains of the DnaJ homologue auxilin. *J. Cell Biol.* 135:925–937.

Honing, S., G. Kreimer, H. Robenek, and B.M. Jockusch. 1994. Receptor-mediated endocytosis is sensitive to antibodies against the uncoating ATPase (hsc70). *J. Cell Sci.* 107:1185–1196.

Jiang, R., B. Gao, K. Prasad, L.E. Greene, and E. Eisenberg. 2000. Hsc70 chaperones clathrin and primes it to interact with vesicle membranes. *J. Biol. Chem.* 275:8439–8447.

Kelley, W.L. 1999. Molecular chaperones: How J domains turn on Hsp70s. *Curr. Biol.* 9:R305–R308.

Kirchhausen, T. 2000. Three ways to make a vesicle. *Nat. Rev. Mol. Cell Biol.* 1:187–198.

Kosaka, T., and K. Ikeda. 1983. Reversible blockage of membrane retrieval and endocytosis in the garland cell of the temperature-sensitive mutant of *Drosophila melanogaster*, *shibire^{ts1}*. *J. Cell Biol.* 97:499–507.

Kramer, H., and M. Phistry. 1996. Mutations in the *Drosophila* hook gene inhibit endocytosis of the boss transmembrane ligand into multivesicular bodies. *J. Cell Biol.* 133:1205–1215.

Lloyd, T.E., R. Atkinson, M.N. Wu, Y. Zhou, G. Pennetta, and H.J. Bellen. 2002. Hrs regulates endosome membrane invagination and tyrosine kinase receptor signaling in *Drosophila*. *Cell.* 108:261–269.

Morgan, J.R., K. Prasad, W. Hao, G.J. Augustine, and E.M. Lafer. 2000. A conserved clathrin assembly motif essential for synaptic vesicle endocytosis. *J. Neurosci.* 20:8667–8676.

Morgan, J.R., K. Prasad, S. Jin, G.J. Augustine, and E.M. Lafer. 2001. Uncoating of clathrin-coated vesicles in presynaptic terminals: roles for Hsc70 and auxilin. *Neuron.* 32:289–300.

Narayanan, R., and M. Ramaswami. 2003. Regulation of dynamin by nucleoside diphosphate kinase. *J. Bioenerg. Biomembr.* 35:49–55.

Newmyer, S.L., A. Christensen, and S. Sever. 2003. Auxilin-dynamin interactions link the uncoating ATPase chaperone machinery with vesicle formation. *Dev. Cell.* 4:929–940.

Newmyer, S.L., and S.L. Schmid. 2001. Dominant-interfering Hsc70 mutants disrupt multiple stages of the clathrin-coated vesicle cycle in vivo. *J. Cell Biol.* 152:607–620.

Pishvaee, B., G. Costaguta, B.G. Yeung, S. Ryazantsev, T. Greener, L.E. Greene, E. Eisenberg, J.M. McCaffery, and G.S. Payne. 2000. A yeast DNA J protein required for uncoating of clathrin-coated vesicles in vivo. *Nat. Cell Biol.* 2:958–963.

Poodry, C.A., and L. Edgar. 1979. Reversible alteration in the neuromuscular junctions of *Drosophila melanogaster* bearing a temperature-sensitive mutation, *shibire*. *J. Cell Biol.* 81:520–527.

Poodry, C.A., L. Hall, and D.T. Suzuki. 1973. Developmental properties of *Shibire*: a pleiotropic mutation affecting larval and adult locomotion and development. *Dev. Biol.* 32:373–386.

Robinow, S., and K. White. 1988. The locus elav of *Drosophila melanogaster* is expressed in neurons at all developmental stages. *Dev. Biol.* 126:294–303.

Rubin, G.M., and A.C. Spradling. 1982. Genetic transformation of *Drosophila* with transposable element vectors. *Science.* 218:348–353.

Rubin, G.M., L. Hong, P. Brokstein, M. Evans-Holm, E. Frise, M. Stapleton, and D.A. Harvey. 2000. A *Drosophila* complementary DNA resource. *Science.* 287:2222–2224.

Schlossman, D.M., S.L. Schmid, W.A. Braell, and J.E. Rothman. 1984. An enzyme that removes clathrin coats: purification of an uncoating ATPase. *J. Cell Biol.* 99:723–733.

Schmid, S.L. 1997. Clathrin-coated vesicle formation and protein sorting: an integrated process. *Annu. Rev. Biochem.* 66:511–548.

Spradling, A.C., D.M. Stern, I. Kiss, J. Roote, T. Laverty, and G.M. Rubin. 1995. Gene disruptions using P transposable elements: an integral component of the *Drosophila* genome project. *Proc. Natl. Acad. Sci. USA.* 92:10824–10830.

Spradling, A.C., D. Stern, A. Beaton, E.J. Rhem, T. Laverty, N. Mozden, S. Misra, and G.M. Rubin. 1999. The Berkeley *Drosophila* Genome Project gene disruption project: single P-element insertions mutating 25% of vital *Drosophila* genes. *Genetics.* 153:135–177.

Sunio, A., A.B. Metcalf, and H. Kramer. 1999. Genetic dissection of endocytic trafficking in *Drosophila* using a horseradish peroxidase-bride of sevenless chimera: hook is required for normal maturation of multivesicular endosomes. *Mol. Biol. Cell.* 10:847–859.

Tomancak, P., A. Beaton, R. Weiszmann, E. Kwan, S. Shu, S.E. Lewis, S. Richards, M. Ashburner, V. Hartenstein, S.E. Celniker, and G.M. Rubin. 2002. Systematic determination of patterns of gene expression during *Drosophila* embryogenesis. *Genome Biol.* 3:research0088.1–0088.14.

Umeda, A., A. Meyerholz, and E. Ungewickell. 2000. Identification of the universal cofactor (auxilin 2) in clathrin coat dissociation. *Eur. J. Cell Biol.* 79:336–342.

Ungewickell, E., H. Ungewickell, S.E. Holstein, R. Lindner, K. Prasad, W. Barouch, B. Martin, L.E. Greene, and E. Eisenberg. 1995. Role of auxilin in uncoating clathrin-coated vesicles. *Nature.* 378:632–635.

van der Bliek, A.M., and E.M. Meyerowitz. 1991. Dynamin-like protein encoded by the *Drosophila shibire* gene associated with vesicular traffic. *Nature.* 351: 411–414.

Wolff, T. 2000. Histological techniques for the *Drosophila* eye. Parts I and II. *In Drosophila* Protocols. W. Sullivan, M. Ashburner, and R.S. Hawley, editors. Cold Spring Harbor Laboratory Press, Cold Spring Harbor, NY. 201–244.

Wucherpfennig, T., M. Wilsch-Brauninger, and M. González-Gaitán. 2003. Role of *Drosophila* Rab5 during endosomal trafficking at the synapse and evoked neurotransmitter release. *J. Cell Biol.* 161:609–624.

Xu, T., and G.M. Rubin. 1993. Analysis of genetic mosaics in developing and adult *Drosophila* tissues. *Development.* 117:1223–1237.

Zhang, Y., B. Grant, and D. Hirsh. 2001. RME-8, a conserved J-domain protein, is required for endocytosis in *Caenorhabditis elegans*. *Mol. Biol. Cell.* 12: 2011–2021.